Low-Dose-Rate Cobalt-60 Testing Results for Kaman KD-5100 Differential Inductive Position Measuring Systems

Bart H. McGuyer, Randall J. Milanowski, and Slaven Moro

***Abstract*—We report ^{60}Co gamma radiation testing of a Kaman KD-5100 position measuring system to a total ionizing dose of 10 kRad(Si) at a rate of 5 mRad(Si)/s.**

I. Introduction

We recently reported the results [1] of 64 MeV proton testing of a commercial position measuring system, the KD-5100 by Kaman Precision Products [2], which has long been used in high-precision applications such as laser beam steering [3], [4]. The proton testing reached a total fluence of 8.6×10^{11} protons/cm^2 and a corresponding total ionizing dose (TID) of 115.7 kRad(Si). We observed and characterized changes in KD-5100 performance with irradiation, including a pronounced recovery/annealing behavior, and presented a model to estimate the combined effects of degradation and annealing for different flux and fluence profiles. The proton data suggest that the KD-5100 will be suitable for space missions with low to moderate TID and displacement-dose requirements, and possibly for missions with more challenging requirements, depending on the position-measurement accuracy required.

Here, we present the results of irradiating a KD-5100 system with ^{60}Co gamma radiation at a low dose rate of 5 mRad(Si)/s up to a TID of 10 kRad(Si) at the Northrop Grumman Corporation Radiation Test Operations (NGC RTO) facility in Redondo Beach, CA. Low-dose-rate exposure to gamma radiation was used to probe for radiation responses associated with bipolar integrated circuit components in the KD-5100 hybrid module. Specifically, the use of gamma radiation eliminates displacement damage contributions to the radiation response, and the use of a low dose rate can reveal Enhanced Low Dose Rate Sensitivity (ELDRS) effects [5], [6]. We hope these results will be of use to the satellite and aerospace industries and will move forward Facebook's goal of extending connectivity.

Manuscript received August 9, 2018.

B. H. McGuyer is with Facebook Inc., 1 Hacker Way, Menlo Park, CA 94025, USA.

R. J. Milanowski is with M&A Inc., 2726 Shelter Island Drive #268, San Diego, CA 92016, USA.

S. Moro is with Facebook Inc., 1 Hacker Way, Menlo Park, CA 94025, USA.

978-1-5090-4647-8/17/$31.00 ©2018 IEEE

II. Part Description and Experimental Approach

The KD-5100 is a high-precision non-contact position measuring system with two measurement channels. Each channel uses a pair of matched inductors as differential sensors to measure the linear displacement or angular tilt of a metal target. The impedance of each sensor depends on the proximity to its target, primarily because inducing eddy currents alters each sensor's self inductance. The KD-5100 measures these impedance changes using an alternating-current balanced bridge circuit similar to a Wheatstone bridge. The bridge output is demodulated and amplified to provide an analog signal that is very nearly linear with changes in the target position. The KD-5100 accomplishes these functions using circuity that includes diodes and bipolar components.

Fig. 1 shows the test system used at the NGC RTO facility. For each measurement channel of the KD-5100 device under test (DUT), the sensor pair was placed about an aluminum

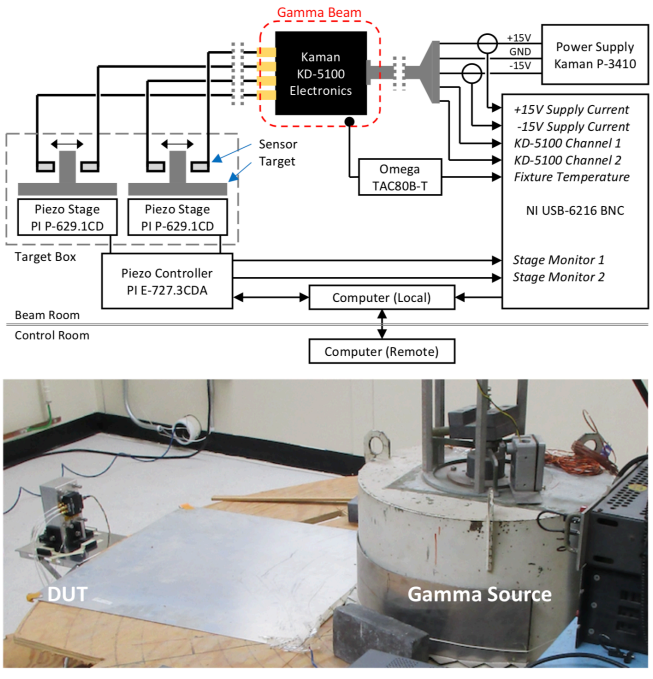

Fig. 1. (Top) Diagram of the test system. (Bottom) Picture of the test system at the NGC RTO facility. Target box and supporting electronics not shown.

target that was controlled by a linear piezo stage. Each piezo stage provided precise control of its target position, and included a capacitive sensor to directly measure its target position. Each sensor pair was installed by offsetting one sensor from a centered target with a precision metal shim, and then adjusting the other sensor to produce a null output [2]. A computer inside the NGC beam room (outside the primary exposure area) controlled the piezo stages and recorded the DUT channel outputs, DUT power supply currents, DUT fixture temperature, and piezo-stage position monitors (capacitive sensor outputs). A separate computer was used to remotely control and monitor the entire test system while at the facility using an Ethernet cable that extended to a control room.

We performed two types of measurements on the DUT at room temperature: active calibrations and passive monitoring. During calibrations, the piezo stages were discretely stepped over a range of 1.5 mm for three to four periods of a triangle wave. The data recorded during a calibration provides a comparison of the DUT outputs and piezo-stage positions, which we use to assess the DUT performance over nearly all of its measurement range. During monitoring, the piezo stages are held fixed by a piezo controller. The target for the first DUT channel is held near one end of full scale, and the target for the second near null. This arrangement makes the first channel mainly sensitive to changes in its gain adjustment, and the second channel mainly sensitive to changes in its null adjustment. Due to improvements, the technical offsets observed during previous proton testing [1] from switching between calibrations and monitoring did not occur here.

We exposed the DUT electronics to ^{60}Co gamma radiation up to a TID of 10.014 ± 0.012 kRad(Si) without interruption as shown in Fig. 2. Here, the TID error includes rate and timing uncertainties but not ^{60}Co source decay. The test setup was installed several days prior to the exposure. We recorded calibration data before and after all irradiation and also during the exposure once each day. Otherwise, we captured passive monitoring data once every 20 seconds throughout the test, with the exception of a brief interruption from computer error.

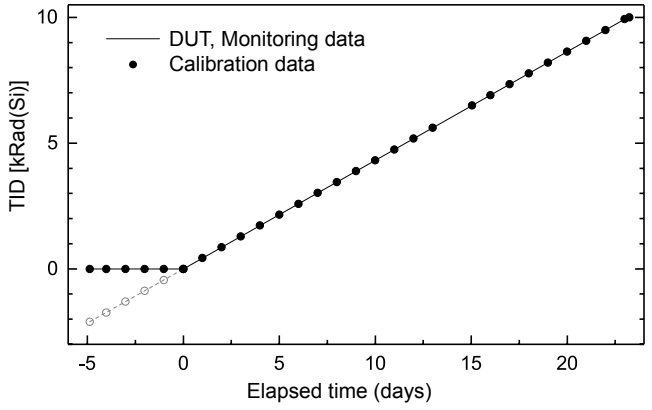

Fig. 2. TID versus time for ^{60}Co gamma irradiation of the DUT. Zero elapsed time marks the start of an exposure at 5 mRad(Si)/s that lasted approximately 23.18 days. Two types of measurements were taken before, during, and briefly after irradiation as shown: monitoring data points every 20 seconds (lines) and calibration data once per day (points). Computer error interrupted both measurements near 6 kRad(Si). The grey dashed line and circles illustrate how in later figures data before irradiation is included for comparison by extending the fixed dose rate to negative TID.

TABLE I
FIT PARAMETERS FOR MONITORING DATA IN FIG. 3 AND GAIN PARAMETERS IN FIGS. 6 AND 7 FROM CALIBRATION DATA, USING THE MODEL (1). VALUES IN PARENTHESIS ARE UNCERTAINTIES IN THE LAST DIGITS FROM LEAST-SQUARES FITTING. THE PARAMETER y_0 IS AN INITIAL VALUE AND x_0 IS A TID THRESHOLD BEYOND WHICH THERE IS A LINEAR EVOLUTION WITH SLOPE $-y_0/D$.

Figure	Data	y_0 (V or V/mm)	x_0 [kRad(Si)]	D [kRad(Si)]
3	Ch. 1	8.51092(1) V	0.9164(9)	543.06(7)
6	G_1	11.1067(7) V/mm	0.71(5)	589(4)
6	G_2	10.9198(7) V/mm	0.77(5)	585(4)
7	G_1'	10.6337(6) V/mm	0.62(6)	624(4)
7	G_2'	10.3961(5) V/mm	0.68(4)	618(3)

III. Experimental Results and Analysis

A. Monitoring Data

Fig. 3 shows monitoring data for the DUT outputs versus time. An interruption from computer error is visible, but the smaller interruptions from calibration data are not visible. As setup, the monitoring data for channel 1 was mostly sensitive to the gain adjustment of that channel and the data for channel 2 to the null adjustment of that channel. The monitoring data is consistent with our previous observation of gain degradation with proton irradiation [1], which is known to occur in bipolar integrated circuits from both displacement damage [7] and certain TID effects [8]–[10].

The data suggests that the effective gain for channel 1 decreased with irradiation approximately linearly for irradiation past a threshold. To model this suspected gain degradation, we fit the channel 1 data with the empirical fit function

$$y(x) = \begin{cases} y_0 & x \le x_0 \\ y_0[1 - (x - x_0)/D] & x > x_0 \end{cases} \quad (1)$$

which models a transition from constant to linear evolution for irradiation x past a threshold x_0. The parameter D models linear gain degradation and is the effective dose after threshold that would lead to zero gain if the linear evolution continued: $y(x_0 + D) = 0$. Table I gives the fit parameters for the data.

Fig. 4 highlights the monitoring data for channels 1 and 2 at the start and stop of irradiation. The data exhibit a transient, oscillatory behavior at the start of irradiation on both channels up to about 0.2 kRad(Si) that is qualitatively similar to behavior observed with a different DUT during the first few minutes of proton irradiation (c.f. Fig.5 of [1]) to a similar dose. However, the timescale here is over several hours instead of minutes, suggesting that if this transient behavior is related, then it is more likely a response to TID than time. At the end of irradiation, the data for channel 1 may possibly indicate the beginning of annealing or recovery behavior, as

was observed with proton irradiation [1]. However, not enough data was taken after irradiation to characterize such behavior.

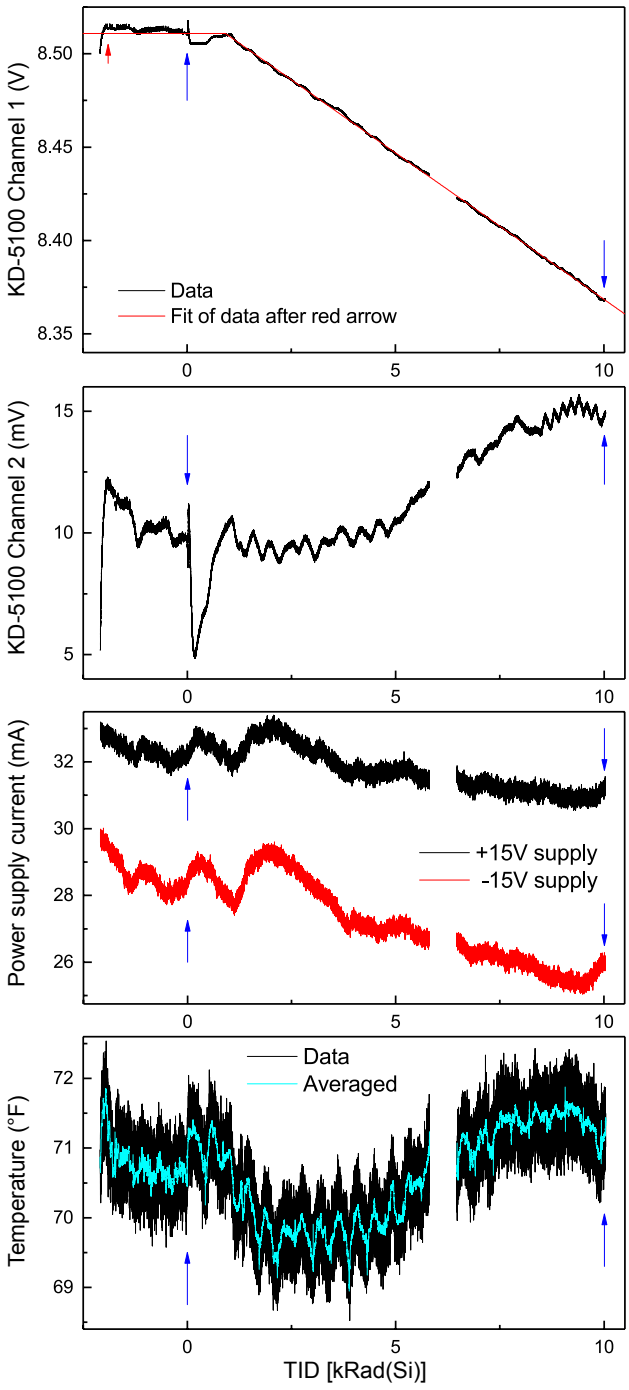

Fig. 3. Monitoring data versus TID. Blue arrows indicate the start and stop of irradiation. Data before irradiation is included for comparison by extending the fixed dose rate to negative TID. The interruption near 6 kRad is from computer error. Channels 1 and 2 exhibited transient behavior at the start of irradiation as well as at the beginning of the data, presumably from thermal and mechanical equilibration of the test setup. The channel 1 data after the red arrow was fit with the model (1) to capture an apparent transition from constant to linear evolution, with fit parameters in Table I. The DUT fixture temperature and the voltage measurement resolution of 0.3 mV may be responsible for some of the observed DUT behavior, in particular, for channel 2.

We did not observe any spikes or other anomalous behavior in the supply currents or the DUT output voltages during exposure. However, before exposure there was anomalous noise measured on channel 1, visible in Figs. 3 and 4, likely due to a poor electrical connection that was resolved prior to irradiation. Fig. 3 includes temperature data for the DUT fixture, as measured and as averaged over 1 hour periods, that is likely responsible for some of the observed transient behavior in Figs. 3 and 4. Likewise, the voltage measurement resolution of 0.3 mV is likely responsible for some of the observed transient behavior in Figs. 3 and 4.

The overall linear trends of the power supply currents are at least partially due to drift of the current probe zero-current readings, which were measured after irradiation stopped to have drifted by -2.3 mA and -3.2 mA for the positive and negative supply probes, respectively. Note that while the power supply currents do vary slightly with target displacement (on the order of ± 1 mA/mm), the target displacements were held fixed during monitoring data.

B. Calibration Data

Fig. 5 shows calibration data from immediately before and after all irradiation. Linear fits to the calibration data of the

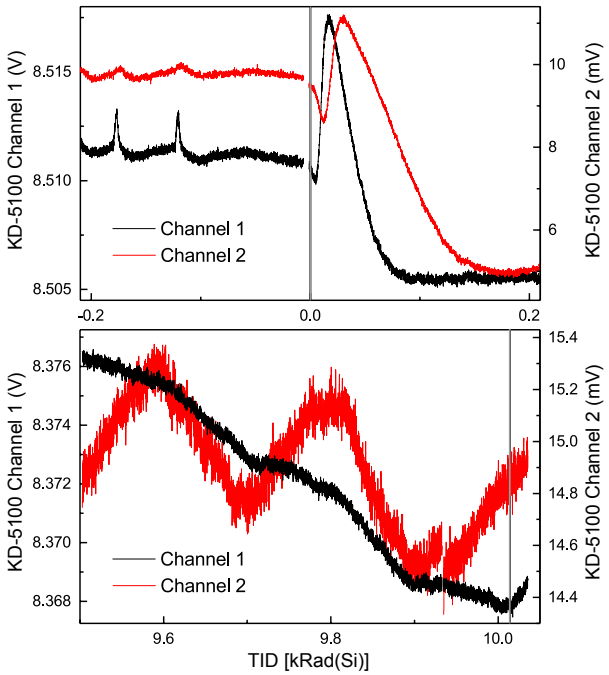

Fig. 4. Finer detail of monitoring data for the DUT outputs near the start and stop of irradiation. Vertical grey lines indicate beam transitions. The transients observed prior to irradiation were likely due to a poor electrical connection that was resolved during the interruption visible before the start. Both channels display an oscillatory behavior after the start of irradiation that is qualitatively similar to behavior observed with proton irradiation [1]. The voltage measurement resolution of 0.3 mV may be responsible for the oscillatory behavior displayed before irradiation stopped. Channel 1 may display a possible onset of annealing/recovery behavior after irradiation stopped, but not enough data was taken to characterize this behavior. The discontinuity near 9.9 kRad for channel 2 is likely from error in reseting the target displacement after a calibration measurement.

TABLE II

LINEAR FIT PARAMETERS FOR SELECT CALIBRATION DATA, INCLUDING THE CURVES IN FIG. 5, FOR COMPARISON WITH TABLE I IN [1]. VALUES IN PARENTHESIS ARE UNCERTAINTIES IN THE LAST DIGITS FROM LEAST-SQUARES FITTING OR ERROR PROPAGATION. THE TID ERRORS INCLUDE RATE AND TIMING UNCERTAINTY BUT NOT SOURCE DECAY. THE PARAMETER Δ_i OF (4) IS AN ESTIMATE FOR THE WORST-CASE ERROR DUE TO IRRADIATION. THE LINEAR FITS WERE OF THE FORM (2).

TID	KD-5100 Channel 1			KD-5100 Channel 2		
[kRad(Si)]	G_1 (V/mm)	N_1 (mV)	Δ_1 (mV)	G_2 (V/mm)	N_2 (mV)	Δ_2 (mV)
0.000	11.107(6)	28(3)	0	10.920(7)	5(3)	0
0.430(1)	11.106(6)	26(3)	−2(6)	10.919(7)	2(3)	−3(7)
1.294(2)	11.098(6)	29(3)	8(6)	10.911(7)	5(3)	8(7)
1.726(2)	11.088(6)	29(3)	18(6)	10.901(7)	5(3)	17(7)
2.590(3)	11.071(6)	29(3)	33(6)	10.885(7)	5(3)	32(7)
5.182(6)	11.021(6)	28(3)	76(6)	10.838(7)	6(3)	76(7)
8.206(10)	10.966(6)	26(2)	125(6)	10.781(7)	9(3)	132(7)
10.014(12)	10.933(5)	24(2)	152(5)	10.747(6)	10(3)	163(6)

form

$$V_i(x) = G_i x + N_i \tag{2}$$

used previously [1] and nonlinear fits of the form

$$V_i(x) = G_i'[(x - x_i) + C_i(x - x_i)^3 + Q_i(x - x_i)^5] + N_i' \tag{3}$$

are shown, where the subscript $i = 1$ or 2 indicates the DUT output channel. For both linear and nonlinear fits, the x values were piezo-stage controller setpoints. Fit residuals included as insets show the nonlinear fit is an improved model for the data.

Figs. 6 and 7 show the fit parameters for all calibration data and their evolution with TID. As with the monitoring data and with previous proton testing [1], the calibration data suggest that the effective gains of each DUT channel decrease with irradiation. Fits of the suspected gain degradation with the model (1) are shown with fit parameters in Table I. The initial data point was excluded from fitting because of suspected thermal and mechanical equilibration of the test setup, to be consistent with the fitting of the monitoring data in Fig. 3.

The form of the nonlinear fit (3) includes the parameters C_i and Q_i to model the leading cubic and quintic nonlinearities expected from differential position measurement. More complicated nonlinearities were observed during proton testing [1] likely from an error in setting the so-called working distances [2] between the sensors and targets. Fig. 7 shows that the fitted values of these parameters are very nearly independent of the gain G_i', which suggests that these nonlinearities likely result more from the physics of the measurement (i.e., sensor and target interaction) than from processing by the KD-5100 circuitry. Excluding the initial data point, which is a suspected outlier as described above, the average values for these parameters were: C_1: 0.1786 ± 0.0008 mm^{-2}; Q_1: −0.1209 ± 0.0008 mm^{-4}; C_2: 0.1938 ± 0.0008 mm^{-2}; and Q_2: −0.1149 ± 0.0008 mm^{-4}.

Select linear fit parameters are included in Table II for comparison with previous proton test data (c.f. Table 1 of [1]). Using the linear fit parameters, Table II and Fig. 6 include the parameter

$$\Delta_i = |N_i - N_i^0| + |1 - G_i/G_i^0| \times (10\ \text{V}) \tag{4}$$

used previously [1] to estimate the worst-case measurement error due to irradiation, where N_i^0 and G_i^0 are the fit parameters for 0 TID.

IV. DISCUSSION

Both DUT channel outputs displayed a brief transient response after the start of irradiation and afterwards an evolution with TID that is consistent with gain degradation. We did not observe any annealing or recovery behavior in the data, or detect related nonlinearity in fits using the model (1), with the exception of a possible onset of such behavior for channel 1 as shown in Fig. 4 after irradiation stopped.

Table I provides a characterization of the suspected gain-degradation response of the DUT, in particular, via the threshold x_0 and slope D parameters of the model (1). The parameter uncertainties are from least-squares fitting and very likely underestimate the variation expected between devices. Table I includes two sets of results for the same calibration data, for which the x_0 parameters agree within error but the D parameters do not. The disagreement with D is due to the difference between the linear (2) and nonlinear (3) fit functions, because nonlinearity in the calibration data influences the gain parameter G_i of the linear fit function. The size of this influence decreases with gain degradation, leading to a steeper slope and thus smaller D for the linear gains. Similarly, the parameters do not agree for the channel 1 monitoring data and G_1. The disagreement for D is due to both the influence of nonlinearities, which led to a smaller D for the monitoring data (c.f. Fig. 5 inset), and the mixture of null and gain contributions in the monitoring data. The disagreement for x_0 is likely due to the influence of transients in the monitoring data and the larger discrete steps between calibration data.

Overall, our observation of gain degradation and initial transients are qualitatively similar with previous proton testing [1], for which the effective dose rate varied between 1.7 to 84.4

Rad(Si)/s. However, proton testing displayed a pronounced annealing/recovery behavior with characteristic exponential decay times of about 11 minutes and 2 hours (c.f. Table II of [1]). The absence of this behavior here is consistent with the empirical model used to characterize it in [1], which numerically suggests that this behavior would not be resolvable here. Alternatively, it is possible that gamma irradiation may not induce annealing/recovery behavior, depending on the mechanism responsible. Additional testing, such as high-dose-rate ^{60}Co testing, would be needed to investigate this further.

Unfortunately, the proton testing observation of annealing/recovery behavior, use of larger steps in TID between calibration data, and inability to combine monitoring data from different exposures make a quantitative comparison of gain degradation difficult. Qualitatively, our observation of a delayed onset near 1 kRad(Si), modeled by x_0 in Table I, is consistent with proton test results (c.f. Table I in [1], in particular, DUT channel 2). Our observation of linearity with TID is consistent with proton testing, which inferred linearity through more than 50 kRad(Si) before the onset of suspected thresholding (nonlinearity) (c.f. Fig. 5 in [1]).

For monitoring data, Table II of [1] provides a characterization of the inferred linear gain degradation. We can compare the proton test results with D in Table I by computing the quantity $-V_0/A$ using the parameters in Table II of [1], which gives 934.9 $\pm$ 0.4 kRad(Si) for DUT channel 1. (The quantity $-V_0/A$ is 1513 $\pm$ 1 kRad(Si) for DUT channel 2, but this channel is expected to be mainly sensitive to the null adjustment, not gain adjustment.) This value for channel 1 is similar to but larger than the values for D observed here, in particular, for DUT channel 1 monitoring data, representing a more gradual degradation for proton testing. However, the

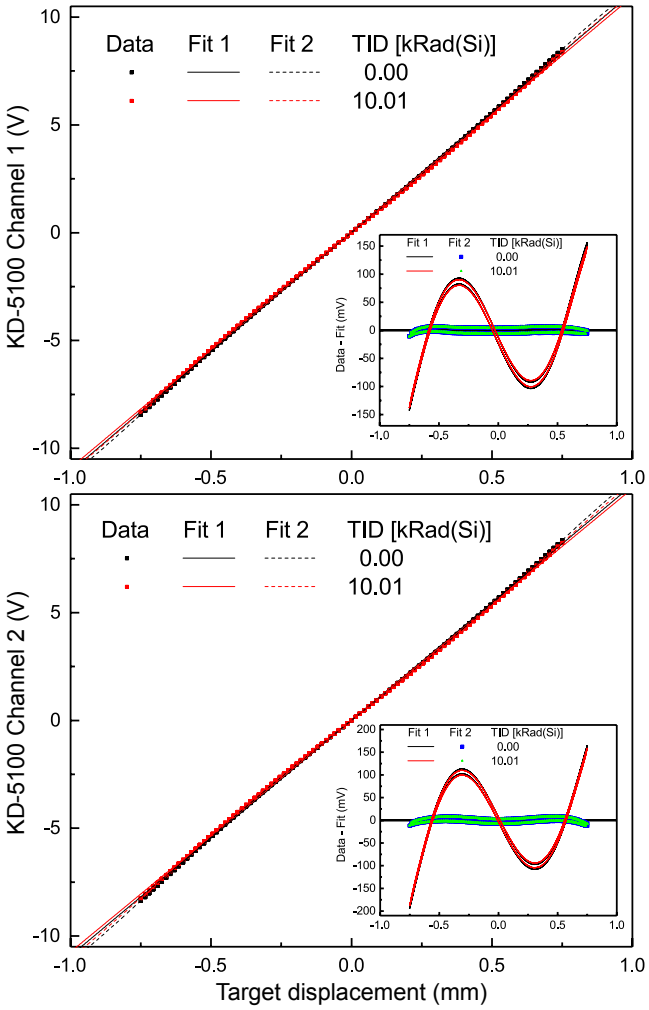

Fig. 5. Calibration data taken before and after ^{60}Co gamma irradiation. Data taken during irradiation is not shown because the curves appear very similar. The solid lines are linear fits of the form (2) with fit parameters listed in Table II. The dashed lines are nonlinear fits of the form (3). Insets show the linear and nonlinear fit residuals, which are representative of all fits to the calibration data. The evolution of the linear and nonlinear fit parameters with TID are shown in Figs. 6 and 7.

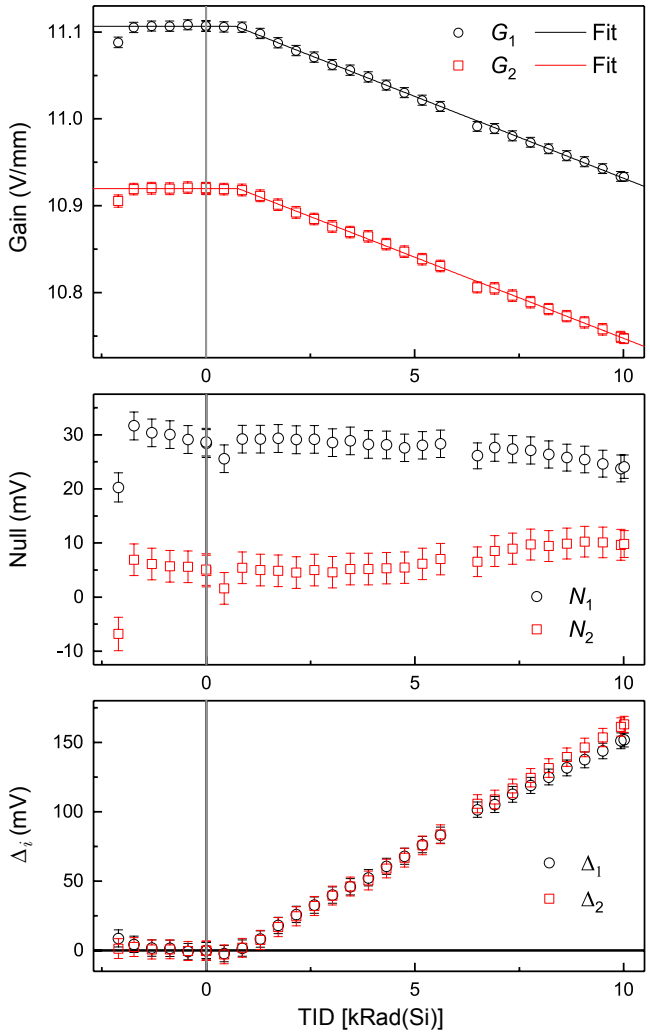

Fig. 6. Evolution of linear fit parameters and derived parameter Δ_i of (4). Data before irradiation is included for comparison by extending the fixed dose rate to negative TID. Select parameters are given in Table II. Fits of suspected gain degradation with the model (1) are shown with fit parameters in Table I. The initial calibration data point was excluded from this fitting because of suspected thermal and mechanical equilibration of the test setup.

quantity $-V_0/A$ characterizes data at higher TID than used here, and the error from removing the influence of simultaneous annealing/recovery behavior is not quantified.

For calibration data, Table I of [1] provides linear fit results of the form (2) for comparison. Unfortunately, there are not enough data points to reliably fit the gain parameters with the model (1). However, fitting the data below 10 kRad(Si) yields an approximate value for D of 523 $\pm$ 85 kRad(Si) for the DUT channels, if the parameter x_0 is artificially varied between 0 and 2 kRad(Si), which is consistent with Table I. Comparing

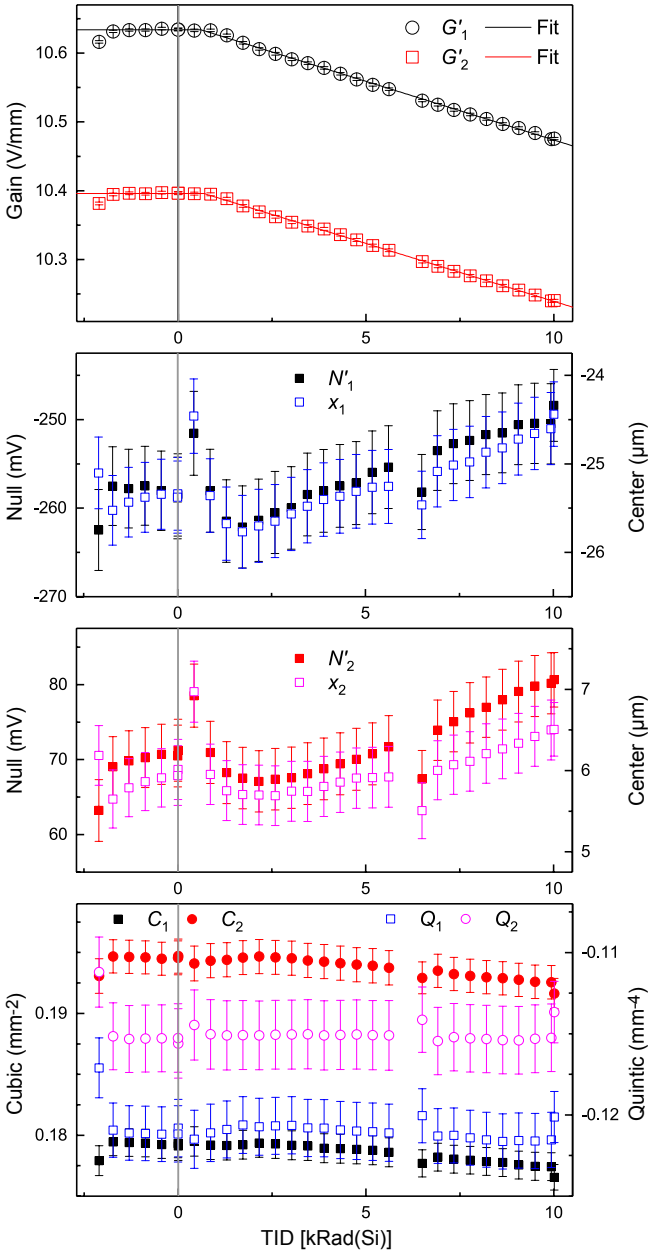

Fig. 7. Evolution of nonlinear fit parameters with irradiation. Data before irradiation is included for comparison by extending the fixed dose rate to negative TID. Fits of suspected gain degradation with the model (1) are shown with fit parameters in Table I. As with the linear fit data, the initial calibration data point was excluded from this fitting.

Table II with Table I of [1], the highest comparable entry is at about 8.2 kRad(Si) TID for both proton and gamma testing. At this TID, the worst-case error estimate Δ_i for proton testing was 157 $\pm$ 5 mV and 148 $\pm$ 3 mV for channels 1 and 2, respectively, while here it was 125 $\pm$ 6 mV and 132 $\pm$ 7 mV.

This experiment probed two possible scenarios with the KD-5100 that are associated with bipolar technology found in some of its components. First, since linear bipolar integrated circuits are sensitive to both ionizing dose and displacement damage, it is possible that protons represent a more damaging environment than gamma radiation for the same TID [11]. However, in cases where the bipolar technologies in a system are significantly prone to ELDRS effects [6], the situation could be reversed and low-dose-rate gamma exposure would represent a more damaging environment than high-dose-rate proton exposure. Comparing the gamma test data here with proton test data [1] suggests that neither scenario dominates the KD-5100 response: Gamma testing produced a slightly smaller degradation in the calibration data (parameter Δ_i) and a somewhat larger degradation in the monitor data (parameters D or $-V_0/A$) than proton testing, as described above.

We note that this comparison deviates from a rigorous application of MIL-STD-883 Method 1019 in two ways. First, we tested a hybrid module which may exhibit complex circuit interactions, whereas 883 Method 1019 is intended for component level application. Second, we compare low-dose-rate ^{60}Co test data with high-dose-rate proton test data, instead of low- and high-dose-rate ^{60}Co test data. This comparison is complicated, in part, by differences in electron-hole pair recombination expected for proton and gamma exposure. Specifically, for a given number of electron-hole pairs produced, more pairs will be lost to high-stopping-power "columnar" recombination (in a proton exposure) than low-stopping-power "geminate" recombination (in a ^{60}Co exposure) [12], [13]. In effect, enhanced recombination in proton exposure may produce a lower effective dose rate. The magnitude of this effect will be larger at lower (several MeV) proton energy, but generally should not invalidate the view of protons as a high-dose-rate source in an ELDRS evaluation, especially for proton energies above about 20 MeV. The proton test data [1] was obtained with 64 MeV (59 MeV after attenuation by DUT packaging) protons which is a high enough energy that the charge yield approaches that of high-energy electrons produced in X-ray and ^{60}Co exposure.

Additionally, we performed a single-event-effects assessment of the active components in the KD-5100 module and concluded, based on part types and technology, that the module presents a low risk for destructive latchup effects.

V. Conclusion

We present the results of low-dose-rate gamma irradiation of a KD-5100 precision position measuring system and compare these results with previous proton test results. The differences observed in gamma and proton testing are smaller than the 2X factor typically applied to TID margins and may be within experimental errors. Overall, the gamma radiation test results

provide increased confidence in the suitability of the KD-5100 for space missions with low to moderate TID requirements.

ACKNOWLEDGMENT

The authors are grateful to Terry Dillahunty and Dean Gacita of Kaman Aerospace Corp. for helpful discussions, Dominic Jandrain for software support, Nick Stephens for computer support, and the Northrop Grumman Corporation Radiation Test Operations for assistance during testing.

REFERENCES

[1] B. H. McGuyer, R. J. Milanowski, S. Moro, N. Hall, and B. Vermeire, "Proton Testing Results for Kaman KD-5100 Differential Inductive Position Measuring Systems," in *2017 IEEE Radiation Effects Data Workshop (REDW)*, July 2017, pp. 1–5.

[2] Kaman Precision Products, "KD-5100 Data Sheet," [Online]. Available: http://www.kamansensors.com/html_pages/KD-5100.html, [Accessed May, 2018].

[3] G. C. Loney, "Design of a high-bandwidth steering mirror for space-based optical communications," *SPIE Active and Adaptive Optical Components*, vol. 1543, pp. 225–235, 1992.

[4] K. R. Lorell and J.-N. Aubrun, "Actively-supported multi-degree of freedom steerable mirror apparatus and method," US Patent 7 009 752, March 7, 2006.

[5] D. Chen, J. D. Forney, R. L. Pease, A. M. Phan, M. A. Carts, S. R. Cox, K. Kruckmeyer, S. Burns, R. Albarian, B. Holcombe, B. Little, J. Salzman, G. Chaumont, H. Duperray, A. Ouellet, and K. LaBel, "The effects of ELDRS at ultra-low dose rates," in *2010 IEEE Radiation Effects Data Workshop*, July 2010, pp. 6–6.

[6] R. L. Pease, R. D. Schrimpf, and D. M. Fleetwood, "ELDRS in bipolar linear circuits: A review," *IEEE Transactions on Nuclear Science*, vol. 56, no. 4, pp. 1894–1908, Aug 2009.

[7] B. G. Rax, A. H. Johnston, and T. Miyahira, "Displacement damage in bipolar linear integrated circuits," *IEEE Transactions on Nuclear Science*, vol. 46, no. 6, pp. 1660–1665, Dec 1999.

[8] D. M. Schmidt, D. M. Fleetwood, R. D. Schrimpf, R. L. Pease, R. J. Graves, G. H. Johnson, K. F. Galloway, and W. E. Combs, "Comparison of ionizing-radiation-induced gain degradation in lateral, substrate, and vertical PNP BJTs," *IEEE Transactions on Nuclear Science*, vol. 42, no. 6, pp. 1541–1549, Dec 1995.

[9] D. M. Schmidt, A. Wu, R. D. Schrimpf, D. M. Fleetwood, and R. L. Pease, "Modeling ionizing radiation induced gain degradation of the lateral PNP bipolar junction transistor," *IEEE Transactions on Nuclear Science*, vol. 43, no. 6, pp. 3032–3039, Dec 1996.

[10] C. Liu, X. Li, J. Yang, G. Ma, and Z. Sun, "Radiation defects and annealing study on PNP bipolar junction transistors irradiated by 3-MeV protons," *IEEE Transactions on Nuclear Science*, vol. 62, no. 6, pp. 3381–3386, Dec 2015.

[11] B. G. Rax, A. H. Johnston, and C. I. Lee, "Proton damage effects in linear integrated circuits," *IEEE Transactions on Nuclear Science*, vol. 45, no. 6, pp. 2632–2637, Dec 1998.

[12] P. Paillet, J. R. Schwank, M. R. Shaneyfelt, V. Ferlet-Cavrois, R. L. Jones, O. Flarrient, and E. W. Blackmore, "Comparison of charge yield in MOS devices for different radiation sources," *IEEE Transactions on Nuclear Science*, vol. 49, no. 6, pp. 2656–2661, Dec 2002.

[13] M. Murat, A. Akkerman, and J. Barak, "Charge yield and related phenomena induced by ionizing radiation in SiO_2 layers," in *2005 8th European Conference on Radiation and Its Effects on Components and Systems*, Sept 2005, pp. PG3–1–PG3–8.